

Self-consistent response of a galactic disc to vertical perturbations

Kanak Saha[†] and Chanda J. Jog

Department of Physics, Indian Institute of Science, Bangalore 560012, India

3 October 2018

ABSTRACT

We study the self-consistent, linear response of a galactic disc to vertical perturbations, as induced say by a tidal interaction. We calculate the self-gravitational potential corresponding to a non-axisymmetric, self-consistent density response of the disc using the Green’s function method. The response potential is shown to oppose the perturbation potential because the self-gravity of the disc resists the imposed potential, and this resistance is stronger in the inner parts of a galactic disc. For the $m = 1$ azimuthal wavenumber, the disc response opposes the imposed perturbation upto a radius that spans a range of 4–6 disc scale-lengths, so that the disc shows a net warp only beyond this region. This physically explains the well-known but so far unexplained observation (Briggs 1990) that warps typically set in beyond this range of radii. We show that the inclusion of a dark matter halo in the calculation only marginally changes (by $\sim 10\%$) the radius for the onset of warps. For perturbations with higher azimuthal wavenumbers, the net signature of the vertical perturbations can only be seen at larger radii - for example beyond 7 exponential disc scale-lengths for $m = 10$. Also, for high m cases, the magnitude of the negative disc response due to the disc self-gravity is much smaller. This is shown to result in corrugations of the mid-plane density, which explains the puzzling scalloping with $m = 10$ detected in HI in the outermost regions $\sim 30\text{kpc}$ in the Galaxy by Kulkarni et al. (1982).

Key words: Galaxies: kinematics and dynamics - Galaxies: spiral - Galaxies: structure

1 INTRODUCTION

Galaxy interactions including interactions with satellite galaxies are now known to be common. As a consequence of such a tidal interaction, vertical distortions in the galactic discs can be easily set in. The most common kind of vertical distortions in discs are warps, corresponding to the azimuthal wavenumber $m = 1$. Tidal interactions with neighbouring galaxies have often been suggested as the mechanism for the origin of warps (Schwarz 1985, Zaritsky & Rix 1997). The generation of the warp of our Galaxy due to the tidal interaction with the Large Magellanic Clouds(LMC) was studied by Hunter & Toomre (1969), and more recently by Weinberg (1995) in the presence of an active dark matter halo. Recent statistical studies by Sanchez-Saavedra et al. (1990) and Reshetnikov & Combes (1998) conclude that at least 50% of all the observed galaxies show warping in their discs. Their study on environmental effects, along with another recent analysis of a large number of edge-on spiral galaxies in the R-band (Schwarzkopf & Dettmar 2001), suggests that tidal perturbation (the $m = 1$ component) plays an important role in generating and influencing large-scale warps.

While it is clear that a warp is more likely to set in in the outer parts of a galaxy where the tidal force is stronger, it is not yet known what decides the actual radius at which a warp starts in the disc. It is a well-known observational fact that warps are seen in the outer regions of galaxies, typically starting at $\sim 4 - 6$ exponential disc scale-lengths, as was first seen in

[†] E-mail : kanak@physics.iisc.ernet.in, cjjog@physics.iisc.ernet.in

2 K. Saha and C.J. Jog

HI observations by Briggs (1990). However there exists no clear physical explanation for the radius at which a warp sets in. In fact, little theoretical attention has been devoted to this question.

Other kinds of vertical distortions that are seen are small-scale corrugations in HI in our Galaxy (Quiroga 1974) or in stars in external galaxies (Florido et al. 1991), and also scalloping in HI in the outer Galaxy (Kulkarni et. al. 1982). Again, the physical origin of these non-axisymmetric features is not understood.

In this paper, we address these questions and show that the self-gravity of the disc resists any vertical distortion, especially in the inner regions. Thus using very general physical principles, we derive semi-analytically a minimum radius for the onset of each of the above vertical perturbations of a galactic disc. Each Fourier component of a perturbing potential will generate its own signature in the galactic disc. Observations of these signatures in the disc depend on the strength of the perturbation component and the disc response corresponding to it. The behaviour of a disc subjected to an external perturbation can entirely be studied by its response function.

We study here the response of an axisymmetric disc, perturbed by a tidal potential and show that the disc self-gravity plays a significant role in sketching a finger-print of the Fourier component of the perturbation onto the disc. We obtain the self-gravitational potential corresponding to a non-axisymmetric, self-consistent, density response of the disc induced by the perturbation component and show that it opposes the perturbing potential. The resulting negative disc response (see Jog 1999 for the planar case) decreases the strength of the perturbation in the disc. The vertical linear disc response obtained here is shown to oppose the perturbation upto a certain radius and for the $m = 1$ component, in particular, it is upto about 4 disc scale-lengths. Thus the net disc response for $m = 1$ or warps can only be seen beyond this radius, which is in a fairly good agreement with observations. We also add a rigid dark matter halo and show that it only marginally affects the location of the onset of warps.

For perturbations with higher azimuthal wavenumbers (m) the disc is shown to be well resistant upto higher radii. In particular we show that any signature of the $m = 10$ component of the perturbation can only be observed in the very outer region of the disc beyond ~ 7 disc scale-length for an exponential disc.

In Section 2, we describe the treatment for the self-consistent linear response of the disc. The results and the comparison with observations are given in Section 3, and the conclusions are summarised in Section 4.

2 VERTICAL DYNAMICS

We study the vertical response in a disc galaxy subjected to a general perturbing potential of $\cos(m\varphi)$ type. We use the cylindrical coordinate (R, φ, z) geometry which is the most natural for describing dynamics in a disc. The dynamical system under study thus consists of a disc embedded in a dark matter halo.

The density distribution of the unperturbed axisymmetric disc is given by

$$\rho_d(R, z) = \rho_{d0} e^{-R/R_d} e^{-|z|/z_0} \quad (1)$$

where ρ_{d0} is the disc central density and R_d is the disc scale-length. z_0 is the vertical scale-height which in general is a function of the galactocentric distance R . In an interacting or merging disc the scale-height z_0 increases systematically with the radial distance. The choice of the double exponential disc comes from a recent study by Schwarzkopf & Dettmar (2001) of tidally-triggered vertical disc perturbations performed on a fairly large sample of disc galaxies which includes both interacting as well as non-interacting galaxies. Their study reports that 33% of the discs show an exponential mass distribution in the vertical direction indicating that most of the disc galaxies prefer to have such non-isothermal vertical profiles. So we are interested in investigating how these non-isothermal discs respond to an external perturbation of the type mentioned above.

The dark matter halo is modeled as an axisymmetric spheroidal system with a pseudo-isothermal density profile which gives an asymptotically flat rotation curve (de Zeeuw & Pfenniger 1988):

$$\rho_h(R, z) = \frac{\rho_{h0}}{1 + (R^2 + \frac{z^2}{q^2})/R_c^2} \quad (2)$$

where ρ_{h0} is the central density of the dark matter halo, R_c is the core radius and q is the halo flattening parameter.

The stars in the disc midplane ($z = 0$) move in a circular orbit at $R = R_0$ with an angular velocity $\dot{\varphi}_0 = \Omega_0$. So the unperturbed circular orbit in the $z = 0$ plane is defined by $R = R_0$ and $\varphi_0 = \Omega_0 t$. The angular velocity Ω_0 is given by

$$\Omega_0^2 = \frac{1}{R_0} \frac{\partial \Psi_0}{\partial R} \Big|_{R=R_0} \quad (3a)$$

where Ψ_0 is the total unperturbed potential:

$$\Psi_{\circ} = \Psi_{d\circ} + \Psi_{h\circ} \quad (3b)$$

$\Psi_{d\circ}$ and $\Psi_{h\circ}$ are connected to the mass distribution described by eq.[1] and eq.[2] respectively through the Poisson equation. $\Psi_{d\circ}$ is given by (see Sackett & Sparke 1990, Kuijken & Gilmore 1989):

$$\Psi_{d\circ}(R, z) = -4\pi G \rho_{d0} R_d^2 z_{\circ} \int_0^{\infty} \frac{J_0(kR)}{[1 + (kR_d)^2]^{3/2}} \frac{k z_{\circ} e^{-|z|/z_{\circ}} - e^{-k|z|}}{k^2 z_{\circ}^2 - 1} dk \quad (3c)$$

A similar calculation for the halo is more cumbersome and we have used the formula given by eq.(2.88) in Binney & Tremaine (1987) to calculate the gravitational force generated by the spheroidal dark matter halo described by the screened isothermal density distribution (eq.[2]).

We consider the perturbing potential at any point (R, φ, z) in the disc due to a perturber at a distance D from the disc centre and at an inclination angle i with respect to the disc midplane:

$$\Psi_1(R, \varphi, z, \Omega_p) = \Psi_{p\circ}(R) \left(1 + \frac{z}{D} \sin i\right) \cos(m\varphi - m\Omega_p t) \quad (4a)$$

The above form of the potential is derived by assuming that $R/D \ll 1$ and $z/D \ll 1$. The form of $\Psi_{p\circ}(R) \sim GM_p R/D^2$ can be taken as a constant in the above limit, where M_p is the mass of the perturber. Ω_p is the pattern frequency of the perturbing potential.

In the present study we consider only the disc response under the perturbing potential with zero-forcing frequency. Generally the zero-frequency response of the disc is much more pronounced than the response generated by a non-zero finite-frequency perturbation (see Terquem 1998 in case of an accretion disc response). Thus the perturbing potential with zero-forcing frequency reduces to

$$\Psi_1(R, \varphi, z) = \Psi_{p\circ}(R) \left(1 + \frac{z}{D} \sin i\right) \cos(m\varphi) \quad (4b)$$

Note that potential of this form in case of $m = 1$ generates a well-defined integral-sign warp in the disc.

The total potential that a disc particle experiences is given by

$$\Psi_{total}(R, \varphi, z) = \Psi_{\circ}(R, z) + \Psi_1(R, \varphi, z) \quad (4c)$$

2.1 Disc linear response:

2.1.1 Basic equations:

The vertical response of a disc to an imposed external perturbation is governed by the following equations. The vertical equation of motion in the small-slope approximation (i.e. for a small deviation from the disc midplane $z = 0$) is given by

$$\frac{d^2 z_m}{dt^2} = -\nu_{\circ}^2 z_m + \left. \frac{\partial \Psi_1}{\partial z} \right|_{(R_{\circ}, \varphi_{\circ}, 0)} \quad (5a)$$

where the vertical frequency due to the unperturbed disc plus halo system is given by

$$\nu_{\circ}^2 = \left. \frac{\partial^2 \Psi_{\circ}}{\partial z^2} \right|_{(R=R_{\circ}, 0)} \quad (5b)$$

The linearized equation of continuity, connecting the perturbed velocity to the perturbed density, is given by (Binney & Tremaine 1987)

$$\frac{\partial \rho_1}{\partial t} + \vec{\nabla} \cdot (\rho_{\circ} \vec{v}_1) + \vec{\nabla} \cdot (\rho_1 \vec{v}_{\circ}) = 0 \quad (6a)$$

We denote $v_1 = v_{zm} = dz_m/dt$ as the perturbed z-velocity and $v_{\circ} = v_{z0}$ as the unperturbed z-velocity. For simplicity we assume $v_{z0} = 0$.

Then the continuity equation (6a) reduces to

$$\frac{\partial \rho_1}{\partial t} + \vec{\nabla} \cdot (\rho_{\circ} \vec{v}_{zm}) = 0 \quad (6b)$$

The response potential corresponding to this perturbed density is connected through the Poisson equation as

$$\nabla^2 \Psi_{resp}(R, \varphi, z) = 4\pi G \rho_1(R, \varphi, z) \quad (7)$$

We solve the above three equations namely eqs.(5a), (6b) and (7) in order to obtain the disc response potential.

On substituting the perturbing potential eq.[4b] into eq.[5a] we obtain a forced oscillator-type second-order differential equation and the solution can be written as

$$z_m = H(R_{\circ}) \cos(m\Omega_{\circ} t) \quad (8)$$

Where

$$H(R_\circ) = \frac{\frac{\partial \Psi_1}{\partial z}|_{(R_\circ, 0)}}{\nu_\circ^2 - \Omega_\circ^2} \quad (9)$$

So the perturbed velocity in the z-direction is given by

$$\vec{v}_{zm} = -m\Omega_\circ H(R_\circ) \sin(m\Omega_\circ t) \hat{z} \quad (10)$$

Substituting this into eq.[6b] and solving for ρ_1 we obtain

$$\rho_1 = -\frac{\partial \rho_\circ}{\partial z} H(R_\circ) \cos(m\Omega_\circ t)$$

Or

$$\rho_1(R_\circ, \varphi_\circ, z) = -\frac{\partial \rho_\circ}{\partial z} H(R_\circ) \cos(m\varphi_\circ) \quad (11)$$

From now on we will use the general co-ordinates (R, φ, z) instead of $(R_\circ, \varphi_\circ, z)$. Note that the unperturbed density distribution for the disc plus the halo system is given by $\rho_\circ(R, z) = \rho_d(R, z) + \rho_h(R, z)$ (from eqs.[1] and [2]). So that after substituting ρ_\circ in eq.[11] we obtain

$$\rho_1(R, \varphi, z) = [\rho_d(R, z) + \zeta_h(R, z)] \left\{ \frac{H(R)}{z_\circ} \right\} \cos(m\varphi) \quad (12)$$

In the above equation $\zeta_h(R, z) = -z_\circ \partial \rho_h / \partial z$ which is a positive quantity for any centrally concentrated self-gravitating system. Since $\partial \Psi_1 / \partial z > 0$ and $\nu_\circ^2 > \Omega_\circ^2$ in an oblate geometry, the function $H(R) > 0$. *Thus the perturbed response density follows the perturbing potential.* This behaviour is generally true for any self-gravitating, centrally concentrated disc (see Section 2.1.2 for details). The total volume density in the disc due to the presence of the m^{th} component of the perturbation can be written as

$$\rho_m(R, \varphi, z) = \rho_\circ(R, z) \left[1 + \left(\frac{\rho_d + \zeta_h}{\rho_\circ} \right) \frac{H(R)}{z_\circ} \cos(m\varphi) \right] \quad (13)$$

2.1.2 Response potential:

The solution of Poisson equation is one of the most tricky issues in this work. Now, the Poisson equation can be solved in two different ways: either by solving the partial differential equation which needs proper boundary conditions to be imposed, or by using the integral equation i.e. using the Green's function method (Jackson 1975). For the planar case, an infinitesimally-thin disc approximation can be used and hence the differential approach could be used (Jog 1999). This approximation is not valid here, and hence this approach cannot be used in the present work. Instead here we have to solve the integral equation using the Green's function method, for which the boundary conditions are directly in-built into the integral equation (Arfken 1985). A compact form of the Green's function in cylindrical coordinates can be found in Cohl & Tohline (1999). We now solve the Poisson equation (eq.[7]) for the non-axisymmetric perturbed density given by eqn(12b) using the Green's function technique. So that

$$\Psi_{resp}(R, \varphi, z) = -G \int_V \frac{\rho_1(\vec{r}')}{|\vec{r} - \vec{r}'|} d^3 r' \quad (14)$$

where

$$|\vec{r} - \vec{r}'| = \left[R^2 + R'^2 - 2RR' \cos(\varphi' - \varphi) + (z' - z)^2 \right]^{1/2}$$

Then

$$\Psi_{resp}(R, \varphi, z) = -G \int_V \frac{\rho_r(R', z') \cos(m\varphi') R' dR' d\varphi' dz'}{[R^2 + R'^2 - 2RR' \cos(\varphi' - \varphi) + (z' - z)^2]^{1/2}} \quad (15)$$

In writing the above equation we have used $\rho_r(R, z) = [\rho_d(R, z) + \zeta_h(R, z)] H(R) / z_\circ$.

After performing the integration over φ' we obtain the response potential corresponding to an odd-m (i.e. $m=1, 3, 5, 7, \dots$) perturbation as

$$\Psi_{resp}^{odd}(R, \varphi, z, m) = -4G \cos(m\varphi) \int_0^\infty \int_{-\infty}^\infty \frac{\rho_r(R', z') R' dR' dz'}{\sqrt{(R + R')^2 + (z' - z)^2}} [2\mathcal{E}_{od}(m, k) - K(k)] \quad (16)$$

where

$$\mathcal{E}_{od}(m, k) = \int_0^{\pi/2} \frac{\sin^2(m\beta)}{\sqrt{1 - k^2 \sin^2(\beta)}} d\beta \quad (17a)$$

and $K(k)$ is the complete elliptical integral of first kind and k is as defined below

$$k^2 = \frac{4RR'}{(R+R')^2 + (z'-z)^2 + z_s^2} \quad (17b)$$

In the above equation, z_s is the small softening parameter added to make the response potential regular at $r = r'$.

Similarly for even- m (i.e., $m = 2, 4, 6, 8, \dots$) perturbation the response potential takes the form

$$\Psi_{resp}^{even}(R, \varphi, z, m) = -4G \cos(m\varphi) \int_0^\infty \int_{-\infty}^\infty \frac{\rho_r(R', z') R' dR' dz'}{\sqrt{(R+R')^2 + (z'-z)^2}} [2\mathcal{E}_{ev}(m, k) - K(k)] \quad (18)$$

where

$$\mathcal{E}_{ev}(m, k) = \int_0^{\pi/2} \frac{\cos^2(m\beta)}{\sqrt{1 - k^2 \sin^2(\beta)}} d\beta \quad (19)$$

Now substituting $\rho_r(R, z)$ into eq.(16) and eq.(18) we obtain

$$\Psi_{resp}^{odd}(R, \varphi, z, m) = -4G \cos(m\varphi) \int_0^\infty \frac{H(R')}{z_\circ} \mathcal{Z}_{exp}^{od}(R, R', z, m) R' dR' \quad (20a)$$

where

$$\mathcal{Z}_{exp}^{od}(R, R', z, m) = \int_{-\infty}^\infty \frac{[\rho_d(R', z') + \zeta_h(R', z')]}{\sqrt{(R+R')^2 + (z'-z)^2}} [2\mathcal{E}_{od}(m, k) - K(k)] dz' \quad (20b)$$

and

$$\Psi_{resp}^{even}(R, \varphi, z, m) = -4G \cos(m\varphi) \int_0^\infty \frac{H(R')}{z_\circ} \mathcal{Z}_{exp}^{ev}(R, R', z, m) R' dR' \quad (21a)$$

where

$$\mathcal{Z}_{exp}^{ev}(R, R', z, m) = \int_{-\infty}^\infty \frac{[\rho_d(R', z') + \zeta_h(R', z')]}{\sqrt{(R+R')^2 + (z'-z)^2}} [2\mathcal{E}_{ev}(m, k) - K(k)] dz' \quad (21b)$$

Using eq.(9) and the definition of the perturbing potential we have

$$H(R') = \Psi_{p\circ}(R') h(R') \quad (22a)$$

where

$$h(R') = \frac{\sin i}{[\nu_\circ^2(R') - \Omega_\circ^2(R')] D} \quad (22b)$$

We assume that $\Psi_{p\circ}(R')$ is a very slowly varying function or even a constant (in agreement with the assumptions in sec 2.) over the disc size and has a small magnitude compared to the background, this is justified since the perturber is typically much more distant than the size of the disc. Thus we can take this term out of the integration in eqs.(20a) and (21a). Then the response potential in the disc midplane($z = 0$) is given by

$$\Psi_{resp}^{odd}(R, \varphi, z = 0, m) = -4G \rho_{d0} \cos(m\varphi) \Psi_{p\circ}(R) \int_0^\infty e^{-R'/R_d} \frac{h(R')}{z_\circ} \mathcal{Z}_{exp}^{od}(R, R', 0, m) R' dR' \quad (23a)$$

and

$$\Psi_{resp}^{even}(R, \varphi, z = 0, m) = -4G \rho_{d0} \cos(m\varphi) \Psi_{p\circ}(R) \int_0^\infty e^{-R'/R_d} \frac{h(R')}{z_\circ} \mathcal{Z}_{exp}^{ev}(R, R', 0, m) R' dR' \quad (23b)$$

Note that the only significant contributions from the dark matter halo to the response potential come through the function $h(R)$ since at the $z = 0$ plane $\zeta_h(R', z')$ part being an odd function of z' contributes zero to the \mathcal{Z} -integrals.

Substituting the perturbing potential at the $z = 0$ plane into eqs. (23a) and (23b), we can write the response potential for the odd- m and even- m perturbations as:

$$\Psi_{resp}^{odd}(R, \varphi, z = 0, m) = \mathcal{R}_m^{odd}(R) \Psi_1(R, \varphi, z = 0) \quad (24)$$

And

$$\Psi_{resp}^{even}(R, \varphi, z = 0, m) = \mathcal{R}_m^{even}(R) \Psi_1(R, \varphi, z = 0) \quad (25)$$

where

$$\mathcal{R}_m^{odd}(R) = -4G \rho_{d0} \int_0^\infty e^{-R'/R_d} \frac{h(R')}{z_\circ} \mathcal{Z}_{exp}^{od}(R, R', 0, m) R' dR' \quad (26)$$

$$\mathcal{R}_m^{even}(R) = -4G\rho_{d0} \int_0^\infty e^{-R'/R_d} \frac{h(R')}{z_o} \mathcal{Z}_{exp}(R, R', 0, m) R' dR' \quad (27)$$

The above eqs.(26) and (27) define the dimensionless response potential of the disc for odd m and for even m perturbations respectively.

The numerical values of the functions $\mathcal{Z}_{exp}(R, R', 0, m)$ are positive for both odd and even m perturbations since at the midplane the dominant contribution from the function $[2\mathcal{E}(m, k) - K(k)]$ (for both even and odd cases) comes when $R = R'$ and $z' = 0$ i.e. $k \sim 1$. The function $h(R)$ is positive in an oblate dark matter halo (since $\nu_o^2 > \Omega_o^2$), whereas it is negative when the dark matter halo is prolate (since $\nu_o^2 < \Omega_o^2$) and the disc self-gravity is negligible. Hence the response function in eqs.(26) and (27) has a negative definite sign for the disc-alone system and also for a system consisting of a disc and an oblate dark matter halo. In contrast, this can have a positive sign for the case of a disc plus a massive prolate dark matter halo. The studies of galactic structure and dynamics in the literature normally assume a spherical halo or an oblate dark matter halo, hence we have performed all our calculations for a nearly spherical halo i.e. with a very small oblateness as a convenient choice.

Thus the dimensionless response potential has a sign opposite to the perturbation potential (eq.[4b]) in the commonly used two cases of disc alone or a disc plus an oblate halo systems. In the linear regime studied here the magnitude of the response potential is proportional to the strength of the perturbation potential. So the resulting disc response potential becomes weaker when the perturber is far away from the disc.

A similar negative disc response in the planar case for a self-gravitating disc was earlier studied in detail by Jog (1999) to explain the radius beyond which lopsidedness is seen in spiral galaxies. In that problem, the disc response to a distorted halo was calculated. We can clearly see that *the negative disc response is a general phenomenon valid for any self-gravitating disc subjected to an external perturbation.*

Note another striking feature that the vertical disc response studied here is independent of the central density ρ_{d0} of the galaxy for a 'disc alone' system and is weakly dependent on the central density $\rho_c = \rho_{d0} + \rho_{h0}$ for a 'disc plus dark matter halo' system. This becomes clear from a close examination of eqs.([26],[27]) and eq.(22b) as $h(R)$ is inversely proportional to ρ_{d0} in the first case, and it depends on ρ_{h0}/ρ_{d0} (which is a small number in general) in the second case. So the behaviour of the disc linear response along the galactocentric distance depends mainly on the three dimensional mass-distribution and depends only weakly on the central brightness of the galaxy. Thus the results obtained below are general and are valid for both normal as well as the low surface brightness galaxies.

2.2 Self-consistent treatment:

In obtaining the disc response potential (see sec.2.1.2) we have ignored the self-gravity of the perturbation itself i.e. the disc response potential was calculated due to the imposed potential alone. Obviously the stars in the disc will be affected by both the externally imposed potential and the potential arising due to the disc response to it. So from the requirement of self-consistency the total potential (Ψ_t) that would be experienced by the disc can be written, following Jog (1999), as:

$$\Psi_t = \Psi_1 + \Psi'_{resp} \quad (28)$$

where Ψ'_{resp} is the self-gravitating potential corresponding to the net self-consistent change in the disc density (ρ') which is obtained as a response to the total potential Ψ_t . Following the argument given by Jog (1999), we can write the total potential experienced by the disc in the presence of an external, linear perturbation as

$$\Psi_t = \chi_m \Psi_1 \quad (29)$$

where

$$\chi_m = \frac{1}{1 + |\mathcal{R}_m(R)|} \quad (30)$$

$\chi_m (\leq 1)$ is called the reduction factor or the susceptibility of the disc in a zero-forcing frequency field. It tells us how the magnitude of the perturbing potential is reduced due to the self-consistent negative disc response. Since $|\mathcal{R}_m(R)|$ is a positive definite quantity, the magnitude of the total perturbed potential in the disc plane is always less than that of the external perturbing potential. In the limiting case of $|\mathcal{R}_m(R)| = 0$ implying $\chi_m = 1$ corresponds to no reduction effect i.e. the disc self gravity plays no role and hence the disc can be taken to be directly exposed to the externally imposed potential.

3 RESULTS:

We study the radial behaviour of different Fourier components (m) of the response potential and investigate its implications for astronomical observations. The basic idea is to find whether there is a pronounced minimum in the response potential and to see if the position of this minimum which we call R_{min} occurs within the typical size of the galactic disc. The net vertical distortion will be seen beyond this radius as argued next.

The net perturbed motion is set by the total potential Ψ_t (eq.[29]) and will decide where a warp is seen. This net perturbed motion is described by eqs.(8) and (9) except that here the perturbation potential Ψ_1 is replaced by the total potential $\Psi_t = \chi_m \Psi_1$ which takes account of the self-consistent response of the disc. Note that the term $1/[\nu_o^2 - \Omega_o^2]$ in equation (9) increases monotonically with radius for any realistic disc galaxy, while χ_m has a minimum at R_{min} . Hence the product of these two terms has a minimum close to R_{min} . Thus the net perturbed motion and hence warp (for $m = 1$) and scalloping (for $m = 10$) will only be seen beyond R_{min} for $m = 1$ and 10 respectively. Therefore, although the response potential and the reduction factor rise on both sides of the minimum (Figs. 1 and 2), the warps will be seen only in the outer parts. This is particularly true in a realistic tidal encounter where the magnitude of the perturbation potential Ψ_{po} will be higher at larger radii whereas here for simplicity we have assumed this to be nearly constant across the disc, see the discussion following eq.(22b).

This has observational relevance if R_{min} occurs within the typical size of a galactic disc as mentioned above. While the optical or stellar disc in a galaxy was long believed to have a sharp outer truncation at 4.5-5 exponential disc scalelengths (van der Kruit & Searle 1981), it has been argued recently on general grounds that the disc can extend beyond this (Narayan & Jog 2003), thus the size of the disc can be larger. In fact, the stellar disc in some galaxies such as NGC 2403 and M33 (Davidge 2003), NGC 300 (Bland-Hawthorn et al. 2005) and M 31 (Ibata et al. 2005), is observed to extend to even 8 or larger disc scalelengths. Thus we are justified in analysing the vertical perturbations to stellar discs upto these radii (Section 3.1).

3.1 $m = 1$ component

The perturbing potential with an $m = 1$ component (as in eq.[4b]), generates the well-known integral-sign warp in a galactic disc. However, so far the physical reason as to where this warp starts in the disc is not understood (Section 1). We try to answer below this question by studying the disc response to the $m = 1$ component of the tidal perturbation.

3.1.1 Radius for onset of warps

The dimensionless response potential (eq.[26]) depends mainly on the ratio of the scale-height to the scale-length z_o/R_d - which we define to be the *thickness parameter* of the disc. This is an important parameter because it provides the information regarding the three-dimensional structure of the disc. A higher value of the thickness parameter indicates a thicker disc, and conversely it is smaller for a thinner disc. It has a weak dependence on the central density of the galaxy in general and in particular for a 'disc-alone' system it is independent of the central density (see Section 2.1). For the sake of simplicity we first treat a constant value of the thickness parameter across the disc.

In Fig.(1), $\mathcal{R}_1(R)$, the response function for the $m = 1$ component is plotted as a function of radius for a constant value of $z_o/R_d = 0.2$ for the disc-alone case and for a disc plus an oblate dark matter halo. The minimum of this response lies within the extent of the optical exponential disc: $R_{min} = 5.6R_d$ for a disc-alone system, while $R_{min} = 5.1R_d$ for the disc plus an oblate-halo system, with halo parameters $R_c = 1.7R_d$, $\rho_{h0} = 0.025$ (in units of M_d/R_d^3) and $q = 0.95$. Thus the inclusion of a rigid halo has a marginal effect on the resulting value of R_{min} , the reason for this is discussed later in this section. Note that these halo parameters are chosen so that they match closely the halo mass model of our Galaxy (see Mera et.al. 1998) and the halo mass, M_h , is $\sim 7M_d$, the disc mass, for these parameters within the total extent of the disc studied ($\leq 10R_d$).

In Fig. 2 we plot the reduction factor χ_1 versus radius, which also shows a minimum close to R_{min} . As discussed above, beyond this radius, the magnitude of the negative disc response decreases, and hence the net disc response increases. Thus the self-gravity of the disc resists a vertical distortion of type $m = 1$ in the inner regions and a net warp is only seen beyond the above R_{min} , which is $\sim 5.1R_d$ for the disc plus oblate-halo case. We note that this lies in the range where warps are seen in galaxies (Briggs 1990).

Varitation with thickness parameter, z_o/R_d :

We have scanned a possible range of the ratio z_o/R_d from 0.05 to 0.5 in case of disc plus an oblate-halo for $M_h \sim 7M_d$ and in all these cases R_{min} lies within $4R_d$ to $6R_d$, see Table 1 below for details. *Thus we show that the warps will be seen beyond a radius in the range of 4-6 R_d , which agrees well with the observed radial range for the onset of warps (Briggs 1990).* This shows that in a normal galaxy disc if warps are generated solely due to the tidal perturbation they are likely to start between 4 - $6R_d$.

Table 1. R_{min}/R_d for $m = 1$ mode vs. Thickness parameter (z_o/R_d)

| (z_o/R_d) | 0.05 | 0.1 | 0.2 | 0.3 | 0.4 | 0.5 |
|---------------|------|-----|-----|-----|-----|-----|
| R_{min}/R_d | 5.9 | 5.6 | 5.1 | 4.7 | 4.4 | 4.2 |

Further note that that as the thickness parameter, z_o/R_d , increases, the resulting R_{min} for the response lies farther in, in the inner region of the disc. The reason for this is that the self-gravity of the disc reduces as the disc becomes puffed up in the vertical direction, hence the net disc distortion can be seen from an earlier radius. This brings out clearly why thin discs have a better resistive power against an external perturbation than the thicker discs.

This physical point has the following implication: if a disc is already heated say due to internal sources such as clouds or spiral arms as in late-type galaxies, then any perturbation of the type considered here (namely the $m = 1$ case) is more likely to disturb it into a warp. Thus a thicker disc is more likely to show warping. This could also be the reason why a larger fraction of galaxies at high redshift are observed to be warped (Reshetnikov et.al. 2002), both because tidal interactions are more likely at high redshift, and these can also heat up a disc, and also because galaxies at high redshift are more gas-rich which can heat up the discs internally.

3.1.2 Implications and Discussion:

Weak Dependence on the halo mass:

Figs. 1 and 2 show that the minima in these and hence the radius for the onset of warps is only marginally affected ($\sim 10\%$) on inclusion of a rigid dark matter halo. This may seem surprising since the halo is known to be dominant in the outer parts. However, there are two reasons for this: first, the disc mass and the halo mass are still comparable to within a factor of few upto the region of interest, namely around R_{min} . Second and more important reason is that the halo density distribution is an even function of z and hence on including the halo, the only change in the disc response function occurs due to the effect on $H(R)$ in eq.[22] (see Section 2.1.2 for details). This weak dependence on the halo mass is highlighted in the next figure.

In Figure 3 we plot the location of the minimum of the response potential, R_{min} , for $m = 1$ vs. M_h/M_d , the ratio of dark matter halo-to-disc mass (where the ratio is obtained for the mass within the size of the disc considered, namely $10 R_d$). The most striking result from this figure is that R_{min} has a weak dependence on the halo-to-disc mass ratio. The value of R_{min} decreases as the halo becomes more and more massive compared to the disc mass. This is because in the presence of a massive halo and hence a higher restoring force, the outer parts of the disc rises gradually as compared to the case of disc alone system where the disc edge bends sharply. We find that R_{min} for the onset of warps is smaller when the disc edge bends more gradually (Fig. 1). This particular result explains well the observational point made by Sanchez-Saavedra et al. (2003) that the farther away the warp stars, the steeper it rises.

So far we have considered the halo to be rigid. An inclusion of a live halo as in a realistic galaxy is much harder to treat without N-body simulations. A live halo would respond to both the direct tidal potential and the perturbed disc configuration. The halo response to the tidal field is shown to magnify the tidal field as seen by the disc and this in turn can increase the amplitude of warp($m=1$)(see Weinberg 1995). So if the live halo forces the disc edge to bend more sharply then we would expect to see an outward-shift in R_{min} . However, in view of the above discussion on R_{min} vs halo mass, we suspect that the location of R_{min} will not be strongly affected in the presence of a live dark matter halo in our problem.

Effect of increasing scale-height, and planar random motion on R_{min} :

The above calculation assumes a constant disc thickness with radius. In a realistic galaxy, the stellar scale-height flares moderately within the optical radius (de Grijs & Peletier 1997, Narayan & Jog 2002). For such a disc where the scale-height or the thickness parameter increases with radius, we find that the resulting values of R_{min} lie slightly within 4 disc scale-lengths. Inclusion of significant planar random motions (which is important for the stellar disc component) in the disc can also shift the R_{min} values in the inward direction. This can be understood from the fact that the planar random motions make the disc stiffer and warp the disc through smaller angles, that is the disc edge bends more gradually, as was shown by Debattista & Sellwood (1999).

These can together explain why many discs show stellar warps (e.g. Reshetnikov & Combes 1998), which therefore must start within the optical radius.

Comparison with Radius of onset for planar lopsidedness:

A thin disc has a stronger self-gravitational force in the vertical direction than in the plane, which explains why the radial distance of 4-6 R_d upto which a disc is able to resist the vertical distortion for the $m = 1$ mode as we have found here, is larger than the disc resistance upto $\sim 2R_d$ to the $m = 1$ mode in the plane (Jog 2000). Thus the idea of negative disc response explains naturally why discs are susceptible to onset of planar lopsidedness from smaller radii as observed (Rix & Zaritsky 1995, Bournaud et al. 2005) while they are able to resist warps till a larger radius (Briggs 1990).

3.2 Higher m components

Perturbations with higher-order azimuthal wavenumbers ($m > 1$) are of particular interest because they may be responsible for producing the corrugations generally seen in the outer region of disc galaxies (Florido et al. 1991). For example for the $m = 4$ component, we find that the minimum of the response potential is at $R_{min} = 6.5R_d$.

The HI gas in the outermost parts of Milky Way shows a remarkable scalloping with a high azimuthal wavenumber $m \sim 10$ (Kulkarni et al. 1982). This interesting feature of the Galactic disc provided us the motivation for studying the response to an $m = 10$ component of the perturbation. The gas surface density is larger than the stellar surface density by about 18 kpc or six disc scalelengths (Narayan et al. 2005), hence the dominant mass component of the disc is HI gas. The treatment for a self-consistent disc response derived in this paper is therefore directly applicable to the gas disc at large radii. For the $m = 10$ case, the minimum of the response potential, R_{min} , occurs at $8.1R_d$ for a disc-alone case, and at $7.1R_d$ for the case of a disc plus an oblate dark matter halo as shown in Fig.4. The dark matter halo parameters used are the same as for Fig.(1).

It is interesting to see that the strength of the dimensionless disc response potential at R_{min} in this case is about 10 times less than that of the $m = 1$ component. But despite its small magnitude, the signature of this higher order perturbation can be clearly seen through the corrugations produced in the midplane density in the outermost part of the disc. In Fig.5 we have shown the resulting isodensity contours of the midplane density perturbed by the $m = 10$ Fourier component of the external perturbation. The contours show a clear deviation from the exponential disc embedded in a screened isothermal dark matter halo beyond 7 disc scale lengths, and the deviation is strong by 10 disc scale-lengths or 30 kpc (assuming $R_d \sim 3$ kpc). This behaviour is in a good agreement with the scalloping with $m = 10$ observed in the outermost regions of HI distribution in the Galaxy (Kulkarni et al. 1982).

4 CONCLUSIONS

This paper shows that the self gravity of the disc resists any vertical distortion in a galactic disc embedded in a dark matter halo. The main results obtained are as follows:

1. We calculate the self-gravitational potential corresponding to a non-axisymmetric, self-consistent density response of the disc, and show that it opposes the perturbation, and this resistance is stronger in the inner parts of a galactic disc. Thus, the net vertical distortion in the disc is only seen in the outer regions. For example, for the $m = 1$ azimuthal wavenumber, the disc response opposes the imposed perturbation upto $\sim 4\text{-}6$ disc scale-lengths, so that the disc shows a net warp only beyond this region. This physically explains the well-known observation that the onset of warps is typically observed beyond this range of radii (Briggs 1990).
2. The net effect of vertical perturbations with higher azimuthal wavenumbers is seen at higher radii. For example, for $m = 10$, the net effect on the disc can only be seen beyond 7 exponential disc scale-lengths and the effect is prominent by 10 disc scalelengths or 30 kpc. The resulting corrugations of the mid-plane density explains the long-known puzzle of scalloping detected in HI at these radii in our Galaxy by Kulkarni et al. (1982).
3. The disc self-gravitational force is stronger along the vertical direction than in the plane. Hence the idea of negative disc response due to the disc self-gravity studied here, and earlier for the planar case (Jog 1999, 2000), naturally explains why discs can resist vertical distortions till a larger radius than the planar ones. This explains why galaxies show net planar lopsidedness from smaller radii (Rix & Zaritsky 1995) compared to the larger radii beyond which warps are seen (Briggs 1990).
4. This paper, plus the earlier work for the planar disc response (Jog 1999, Jog 2000), shows that the inner regions of discs are robust and able to resist a distortion as say induced by tidal interactions. This is a general result and is valid for any disc or a disc plus halo system subjected to an external perturbing potential. This result could be important in the gradual build-up of galactic discs now being studied in cosmological scenarios.

Acknowledgements: We are grateful to the anonymous referee for very useful and constructive comments, particularly regarding the inclusion of a dark matter halo. K.S. would like to thank the CSIR-UGC, India for a Senior research fellowship.

References

Arfken, G. 1985, Mathematical Methods for Physicists (New York: Academic)

Binney, J. & Tremaine, S. 1987, Galactic Dynamics (Princeton: Princeton Univ. Press)

Bland-Hawthorn, J., Vlajic, M., Freeman, K.C., & Draine, B.T. 2005, *ApJ*, 629, 239

Bournaud, F., Combes, F., Jog, C.J., & Puerari, I. 2005, *A & A*, 438, 507

Briggs, F. 1990, *ApJ*, 352, 15

Cohl, H. S., & Tohline, J. E. 1999, *ApJ*, 527, 86

Davidge, T.J. 2003, *AJ*, 125, 3046

de Grijs, R. , & Peletier, R.F. 1997, *A & A*, 320, L21

de Zeeuw, T., & Pfenniger, D. 1988, *MNRAS*, 235, 949

Debattista, V.P., & Sellwood J. 1999, *ApJ*, 513, L107

Hunter, C., & Toomre, A. 1969, *ApJ*, 155, 747

Florida, E., Battaner, E., Sanchez-Saavedra, M. L., Prieto, M., & Mediavilla, E. 1991, *MNRAS*, 251, 193

Ibata, R., Chapman, S., Ferguson, A.M.N., Lewis, G., Irwin, M., & Tanvir, N. 2005, *ApJ*, 634, 287

Jackson, J. D. 1975, Classical Electrodynamics (New York: Wiley)

Jog, C. J. 1999, *ApJ*, 522, 661

Jog, C. J. 2000, *ApJ*, 542, 216

Kuijken, K., & Gilmore, G. 1989, *MNRAS*, 239, 571

Kulkarni, S. R., Blitz, L., & Heiles, C. 1982, *ApJ*, 259, L63

Mera, D., Chabrier, G., & Schaeffer, R. 1998, *A & A*, 330, 953

Narayan, C.A., & Jog, C.J. 2002, *A & A*, 390, L35

Narayan, C.A., & Jog, C.J. 2003, *A & A*, 407, L59

Narayan, C.A., Saha, K., & Jog, C.J. 2005, *A & A*, 440, 523

Quiroga, R. J. 1974, *Ap & SS*, 27, 323

Reshetnikov, V., & Combes, F. 1998, *A & A*, 337, 9

Reshetnikov, V., Battaner, E., Combes, F., & Jimenez-Vicente, J. 2002, *A & A*, 382, 513

Rix, H.-W., & Zaritsky, D. 1995, *ApJ*, 447, 82

Sanchez-Saavedra, M. L., Battaner, E., & Florida, E. 1990, *MNRAS*, 246, 458

Sanchez-Saavedra, M. L., Battaner, E., Guijarro, A., Lopez-Corredoira, M., & Castro-Rodriguez, N. 2003, *A & A*, 399, 457

Sackett, P., & Sparke, L. 1990, *ApJ*, 361, 408

Schwarz, U. J. 1985, *A & A*, 142, 273

Schwarzkopf, U., & Dettmar, R.-J. 2001, *A & A*, 373, 402

Terquem, C. 1998, *ApJ*, 509, 819

van der Kruit, P., & Searle, L. 1981, *A & A*, 95, 105

Weinberg, M. D. 1995, *ApJ*, 455, L31

Zaritsky, D., & Rix, H. -W. 1997, *ApJ*, 477, 118

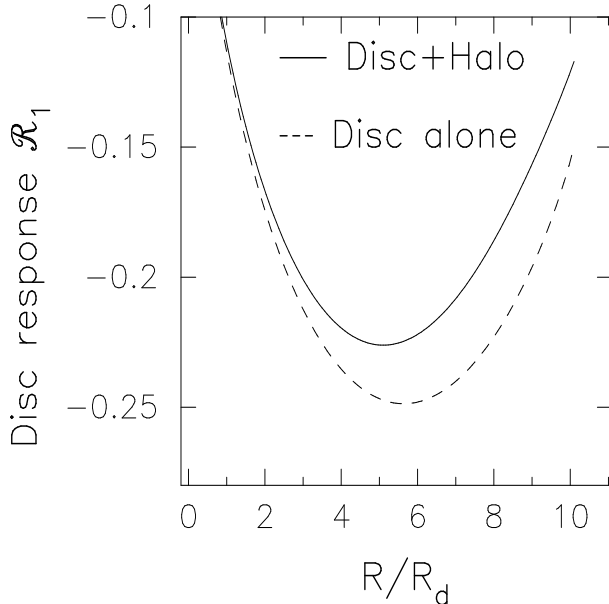


Figure 1. Dimensionless response potential, \mathcal{R}_1 for the $m = 1$ Fourier component of the external perturbation for a constant thickness disc. The scale-height to scale-length ratio i.e. z_0/R_d is taken to be 0.2. This figure shows that R_{min} occurs at $5.6R_d$ for the disc-alone system and at $5.1R_d$ for the disc plus halo system.

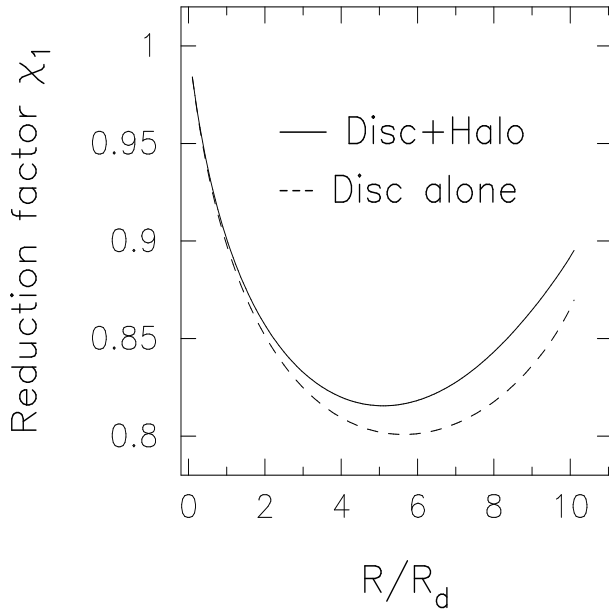


Figure 2. Reduction factor χ_1 for the $m = 1$ component of the perturbation potential due to the negative disc response for $z_0/R_d = 0.2$. The minimum of the reduction factor occurs at a radius $R_{min} = 5.6R_d$ for the disc-alone system and at $5.1R_d$ for the disc plus halo system. Beyond R_{min} , the reduction factor increases steadily.

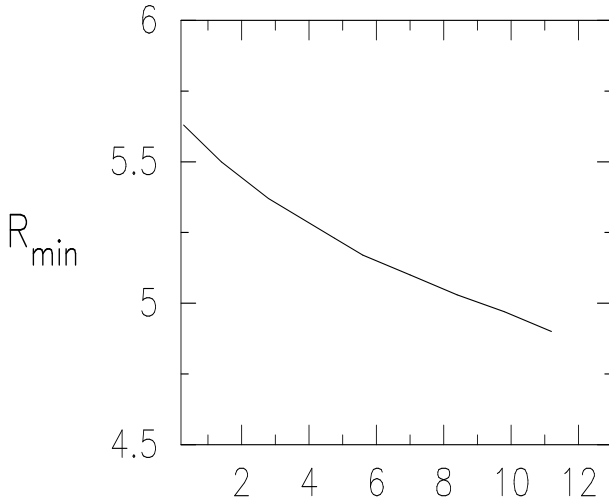


Figure 3. R_{min} for the response potential of $m = 1$ vs. the ratio of the dark matter halo to disc mass, considered within the radius of $10R_d$. The figure shows that the R_{min} has a weak dependence on M_h/M_d , the halo-to-disc mass ratio.

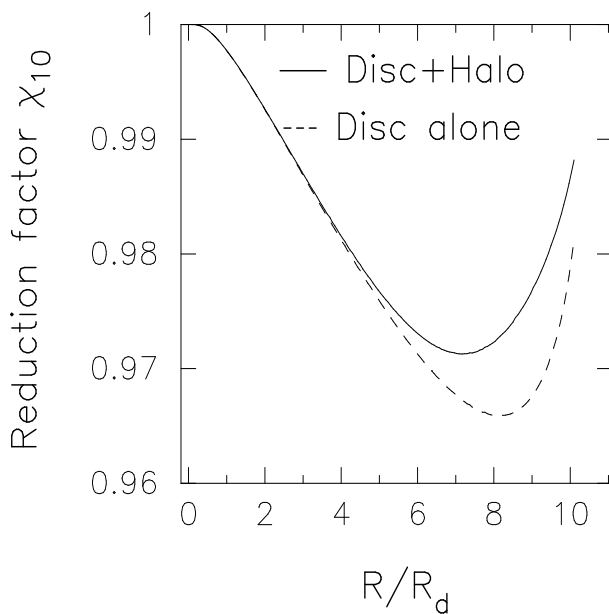


Figure 4. Reduction factor χ_{10} for $m = 10$ Fourier component of the external perturbation, calculated for $z_o/R_d = 0.2$. R_{min} of the response is located at $7.1R_d$ and $8.1R_d$ for a disc plus halo system and a disc-alone system respectively. The reduction factor increases sharply beyond these radii. Note that the reduction due to the negative disc response is very small in magnitude compared to that for the $m = 1$ case.

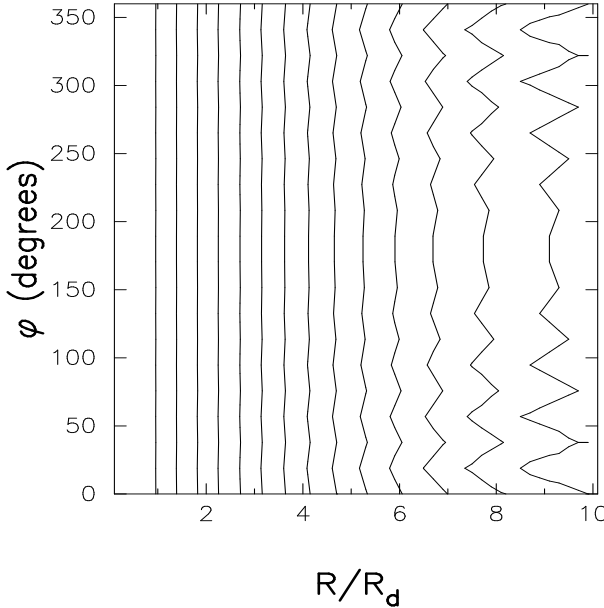


Figure 5. Contour diagrams for the disc mid-plane density perturbed by the $m = 10$ Fourier component of the perturbation in the (R, φ) plane. The mass of the perturber is taken to be 10% of the disc mass and at a distance ~ 36 kpc (for $R_d \sim 3$ kpc) from the disc centre. Contour levels are $\rho_c \times (0.408, 0.272, 0.181, 0.12, 0.08, \dots)$; where ρ_c is the total central mid-plane density of the galaxy in $M_\odot pc^{-3}$. Contours after 7 disc scale-length deviate clearly from the unperturbed midplane mass distribution and the deviation is stronger by ~ 10 disc scale-lengths or 30 kpc, showing the signature of scalloping.